DOI: 10.37190/abb/206939

Numerical Reconstruction Of A Minivan-Pedestrian Collision Using A Chinese Pedestrians Model For Injury Analysis

Jiapeng Li[1], Yu Liu[1*], Huida Zhang[1], Xiaofan Wu[1], Kexin Huang[1], Guibing Li[2], Jiaqi Qian[3]

[1] China Automotive Engineering Research Institute Co Ltd, Chongqing, China
[2] School of Mechanical Engineering, Hunan University of Science and Technology, Xiangtan, China
[3] The State Key Laboratory of Advanced Design and Manufacturing Technology for Vehicle, Hunan University, Changsha, China
*Corresponding author: Yu Liu, China Automotive Engineering Research Institute Co Ltd, Chongqing, China, e-mail address: liuyu@caeri.com.cn

Submitted: 25th February 2025

Accepted: 10th June 2025

Abstract

Purpose

The objective of this study is to numerically reconstruct a collision between a minivan and a pedestrian, and to reproduce the injury conditions of the pedestrian's head, chest, and lower extremities. This research aims to provide a reference for the numerical reconstruction studies of traffic collisions based on human body models.

Methods

The walking posture of the Chinese 50th percentile male pedestrian model AC-HUMs (Advanced China Human body Models) is transformed, after which an analysis model is established for simulation based on the simplified model of the minivan vehicle and the collision information. Subsequently, the injury conditions of the model's lower extremities, chest, and head are extracted and compared with the information of the injured person.

Results

The findings reveal that the pedestrian model exhibits tibia-fibula fractures in the lower limbs, six rib fractures in the chest, and a head injury classified as AIS5 (Abbreviated Injury Scale), suggesting a potential risk of concussion. While the injuries to the lower limbs and chest are predicted with considerable accuracy, the head injuries in the model are more severe.

Conclusions

In the reconstruction of a minivan-pedestrian collision using the AC-HUMs model, AC-HUMs showed good injury-prediction capabilities for the pedestrian's lower limbs and chest, and while the head injury prediction based on intracranial pressure was more severe, that based on brain strain was consistent with the actual situation, reflecting the model's satisfactory performance. This research provides valuable insights for studying injury patterns among Chinese pedestrians through numerical reconstruction.

Keywords

numerical reconstruction, Chinese anthropometric pedestrian model, pedestrian collisions, injury analysis

1 Introduction

It is demonstrated by the statistics of the World Health Organization (WHO) that approximately 1.35 million people lose their lives in traffic collisions worldwide each year, among which the proportion of vulnerable road users (VRU) exceeds half [20]. The data from 2011 to 2023, sorted out by the China In-Depth Accident Study (CIDAS), reveals that the proportion of accidents involving collisions between passenger cars and VRU is extremely high, reaching 83.41%. Pedestrians as a particularly vulnerable group in traffic lack adequate protection and often suffer severe injuries when involved in collisions. Statistical data reveal that pedestrians account for 37.18% of fatalities in passenger car collisions which is the highest proportion among all categories [3].

Many scholars have conducted summaries regarding research on pedestrian collisions. Simms [4] summarized the injuries of pedestrians, kinematic characteristics, and other aspects in pedestrian collisions, as well as related content such as common pedestrian injury mechanisms. The research indicates that although in less developed regions like South America and Africa, the proportion of pedestrian casualties in traffic collisions is significantly higher than that in developed countries and regions. In terms of the injury distribution, the proportion of lower limb injuries is the highest, exceeding 32%, followed by injuries to the head and chest. However, the injury levels involving pedestrians usually do not exceed AIS3.

It is recognized from the pedestrian injury sites [23] that head injuries are identified as the primary cause of pedestrian deaths, representing approximately 49%, while chest injuries are noted as the second leading cause, accounting for around 22%. In pedestrian collisions, the lower limbs (including the pelvis) are observed to have the highest injury incidence, at about 40%, and the head injury incidence is recorded at approximately 31%. Consequently, the lower limbs, head, and chest are highlighted as the body regions that endure more severe injuries in pedestrian collisions and should be prioritized in the research of pedestrian injuries [12].

Numerical simulation through the use of the finite element model is regarded as an important means for conducting collision reconstruction work and exploring the mechanism of pedestrian injuries. When compared with the multi-body dynamics analysis method [13], it is recognized to enable in-depth analysis of injuries to various parts of the body. It is commonly practiced to utilize a single model, such as a lower limb model or a head model, to analyze pedestrian collisions. For instance, in Wang's study [19], a lower limb model was utilized to predict long bone fractures in bus-pedestrian collisions in real accidents. However, these studies are noted to focus solely on specific body regions and employ a single model of the corresponding body part. The constraints imposed by other body parts are acknowledged to influence the kinematics and injuries of the target body region. For example, the constraint of the neck on the head [1] and the mass of the trunk and lower limbs [6] are considered to affect the response of the head. Therefore, it is concluded that the utilization of a complete human body model for collision reconstruction work is deemed more rational.

Daniel Wdowicz [24] reviewed the numerical simulation studies of pedestrian-involved accidents and indicated that a typical pedestrian collision accident can be divided into three stages. The contact stage occurs between the first collision of the pedestrian (usually the lower limbs) and the separation of the pedestrian from the vehicle. The flight stage is from the moment of the separation of the pedestrian and the vehicle to the moment of the first contact with the ground. The sliding stage starts from the moment when the pedestrian first touches the ground, through bouncing, sliding, or rolling, until coming to a complete stop. Numerical reconstruction work often focuses on the first stage, which is usually influenced by the vehicle collision speed and the braking intensity.

In addition, the front-end structure of the vehicle (such as the height of the vehicle's center of mass, the relative position of the bumper, etc.) and the relative position between the vehicle and the pedestrian are important factors affecting pedestrian kinematics. To this end, Mariusz [15] proposed a method for predicting pedestrian kinematics, which can effectively predict the kinematic parameters of pedestrians when they are involved in collisions with SUV (Sport Utility Vehicle) models.

The utilization of the Total Human Model for Safety (THUMS) model for numerical reconstruction work is widely recognized as a prevalent method [2], [10], [25]. A study conducted by Wang et al. [20] on the mechanism of pedestrian lower limb injuries employed the THUMS pedestrian model and a simplified car model. It was revealed that collision speed and collision position have a substantial impact on pedestrian lower limb injuries. However, it was noted that the vehicle model used was overly simplified, and only lower limb injuries could be investigated, while other injuries, such as head injuries, were not explored. In relation to lower limb injuries, Pal et al. [14] compared the influence of the relative height of the vehicle and the pedestrian lower limb on pedestrian lower limb injuries using a scaled pedestrian model. The results indicated that the relatively higher the vehicle, the greater the risk of pelvic and femoral injuries to pedestrians. In Chen's study [3], significant differences were discovered in the speeds of pedestrian heads of different body sizes when they come into contact with the vehicle, with the maximum difference exceeding 30% (between children and 95th percentile men), which subsequently leads to differences in head injuries. According to Watanabe's study [22], during the process of pedestrian collisions, the forces on heads of different body sizes were found to differ by nearly 200%, and the forces on the chest differed by more than 150%. In this study, small-sized pedestrians were consistently observed to be at a disadvantage in pedestrian collisions.

Numerous studies have been conducted using pedestrian models based on European or American anthropometric data. However, there is a notable paucity of research regarding accident scenarios involving the Chinese population. Based on the above studies, it can be concluded that body size differences have a significant influence on pedestrian injury characteristics. Therefore, it is deemed essential to conduct research based on human body models in Chinese anthropometry.

The objective of this numerical reconstruction is to adjust the posture of the Chinese human body model AC-HUMs based on the vehicle injury scenario, ultimately restoring the collision conditions. The injuries to the lower limbs, head, and chest of the AC-HUMs model are compared with the injury reports of the affected individual. The injury reconstruction results are utilized to evaluate the injury prediction capability of AC-HUMs and to explore the injury mechanisms of pedestrians when struck by minivan. This study is intended to serve as a reference for research on Chinese pedestrian injuries using numerical reconstruction (Figure 1).

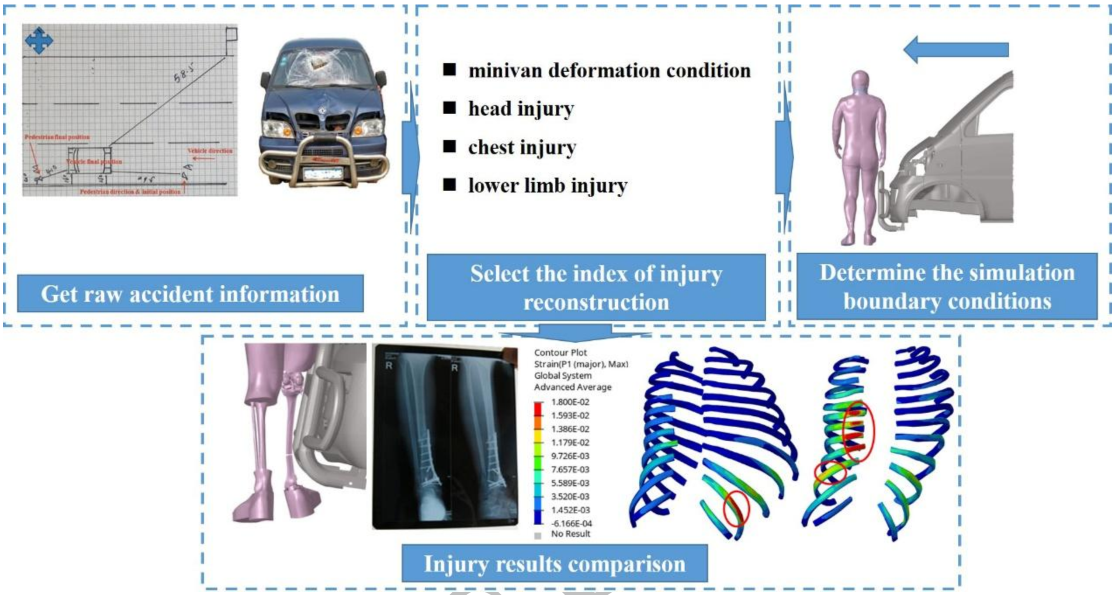

Fig. 1. Numerical reconstruction process based on real accident

2 Methods

2.1 Introduction to human body model

The model utilized in this study is the AC-HUMs model, representing a 50th percentile Chinese male pedestrian. This model incorporates the primary structures of the human body, including detailed cranial structures, spinal components, thoracic and abdominal organs, sternum and ribs, limb bones, and ligaments (Figure 2). The cranial skull of the model features a sandwich structure, a brain-skull sliding interface, and detailed partitioning of brain tissue, ensuring a high degree of fidelity in representing the human head. Within the chest and abdomen, a rotational hinge structure has been implemented, along with detailed modeling of thoracic and abdominal cavity organs. The neck of the AC-HUMs model includes solid element muscles and active muscle forces. Detailed joints and ligaments have been established in the upper and lower limbs, and all long bones are modeled using hexahedral elements to ensure computational accuracy (Figure 2).

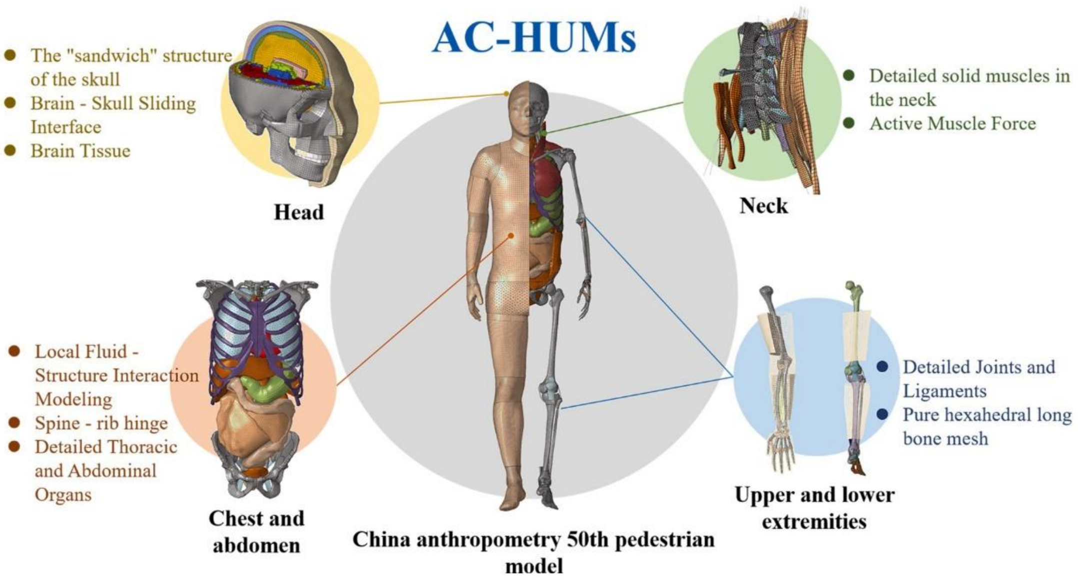

Fig. 2. AC-HUMs M50 pedestrian model

The materials of theAC-HUMs are similar to those of THUMS [18]. For example, the bone components are modeled as elastoplastic materials, while the soft tissues are modeled as hyperelastic materials. Ligaments usually exhibit low stiffness for slight elongation rates but high stiffness for significant elongation rates. Organs with solid structures, such as the liver and kidneys, have incompressible mechanical characteristics. The hyperelastic material model accurately simulates the mechanical behavior of soft tissues, including the skin and muscles. However, hollow organs such as the lungs and intestines have compressible mechanical properties and are therefore considered to be made of low-density foam materials.

Each component of the model has been rigorously validated and demonstrates excellent biomechanical fidelity. For instance, the impact mechanical response and translational and rotational kinematics of the head have been verified, and the facial structure has undergone rod impact and disc impact validation. The neck has been subjected to axial tensile loading mechanical verification and slip table kinematic validation. For the chest and abdomen, impact validation and seatbelt loading verification have been conducted to assess their fidelity. Dynamic and quasi-static loading verification has been performed on the organs to ensure the biomechanical accuracy of key structures. Long bones have been validated through three-point bending tests, and joints have been verified through impact testing. Additionally, kinematic validation of the pedestrian model has been performed, with all results falling within a reasonable range (Figure 3, Figure 4, Figure 5).

The AC-HUMs 50th percentile male model measures approximately 170.7 cm in height and weighs 68 kg. When compared to the THUMS 50th percentile male model [18], its body size is more representative of the injured individual in this study. The AC-HUMs model was initially positioned in the TB024 posture [5] for this accident reconstruction. To accurately simulate the impact postures of the head, chest, abdomen, pelvis, and lower limbs (left and right legs), the upper body trunk of the pedestrian model was pre-simulated to lean forward by 3°, and the right leg was adjusted backward by 7° using a pre-simulation method (Figure 6). To account for the greater deformation observed on the left side of the minivan bumper compared to the right side, the limb positions of the AC-HUMs model were reversed (changing from the left foot forward and right foot backward to the right foot forward and left foot backward).

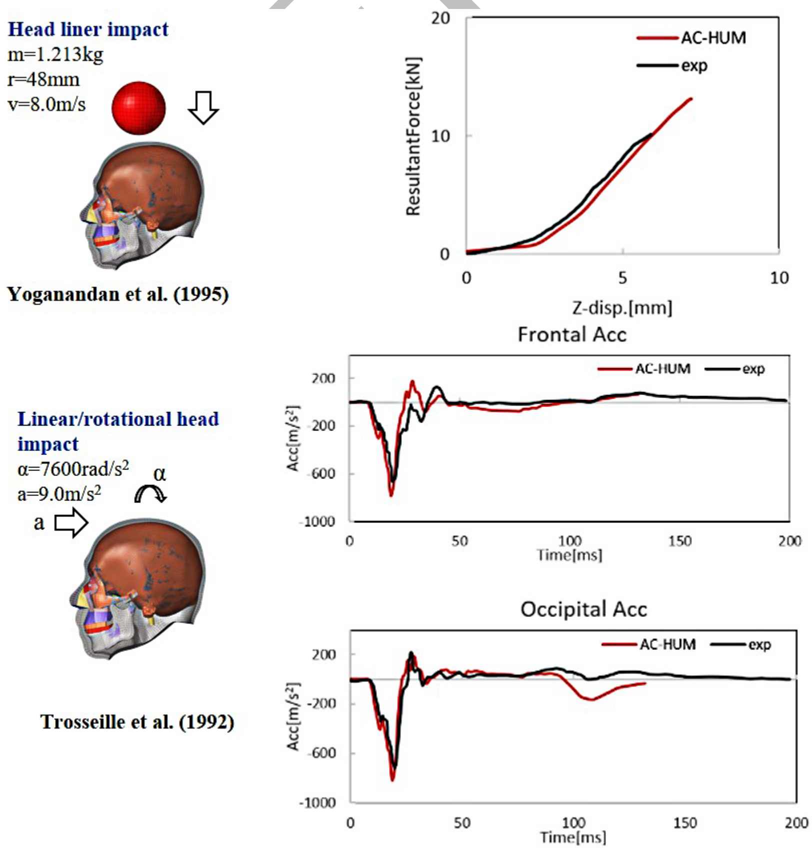

Fig. 3. Part verification of AC-HUMs head model

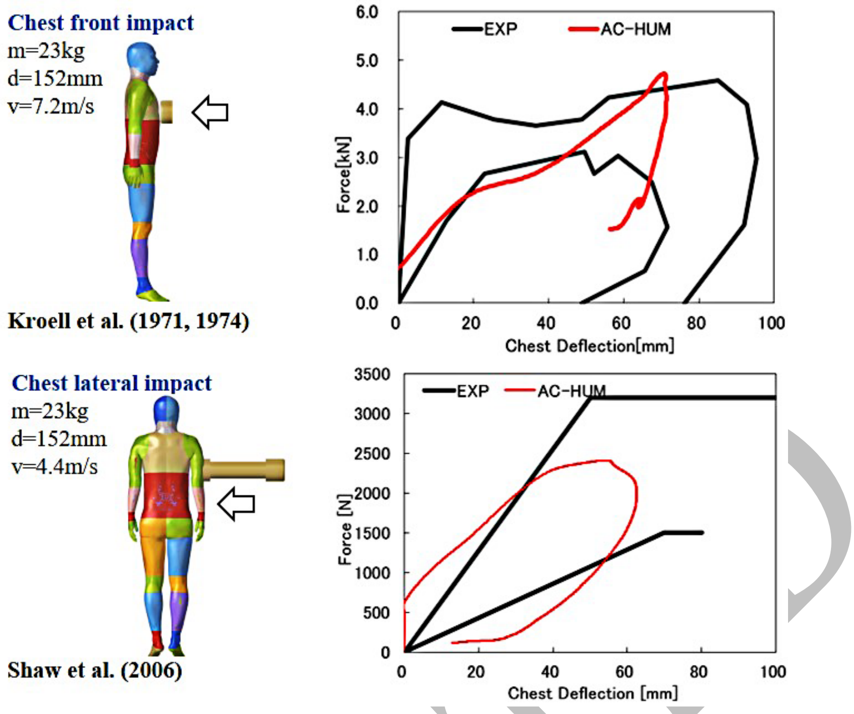

Fig. 4. Part verification of AC-HUMs chest model

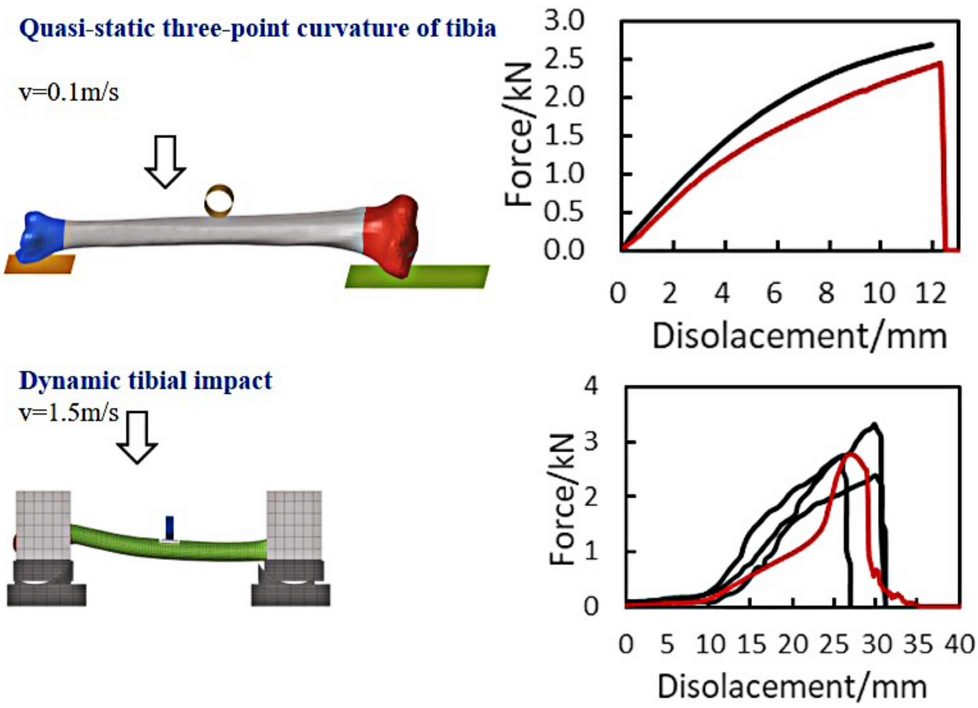

Fig. 5. Part verification of AC-HUMs lower extremity model

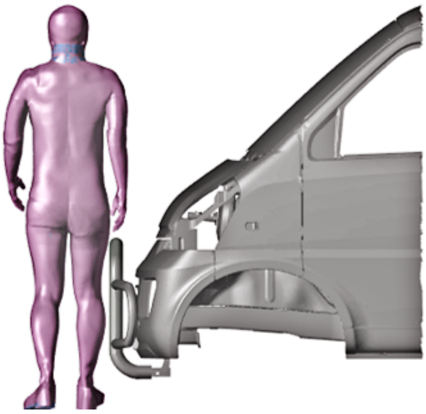

Fig. 6. Initial collision position of the analytical model

2.2 Accident information

In this study, a case of a collision between a minivan and a pedestrian was chosen. The collision was detected in China by the Investigation of Car Accidents in Changsha (IVAC) working group. It was a typical pedestrian - related accident where the victim was knocked down from the right by a moving minivan when crossing the road [9] (Figure 1). In this instance, a pedestrian, who was approximately a 50th percentile male in China, was hit by a minivan. The right side of the injured individual was engaged in the collision. The impact location was close to the center of the minivan, and three significant deformations were shown by the minivan. The impact speed was measured at 45 km/h, and the friction coefficient between the pedestrian and the ground was determined to be 0.7 [8]. The rest of the collision - related information, such as minivan details, pedestrian details, and pedestrian injuries, has been presented (Table 1).

The collision velocity was obtained according to the multi-body dynamics studied by Li[8] and interviews with drivers, $v = 3.6*2\ \mu g L^{1/2}$: v is the impact speed in km/h, μ is the friction coefficient = 0.7 for dry road surface, $g = 9.8\ m/s^2$ and L is the breaking distance.

Table 1. Summary of the collision case [8]

Item	Category	Details	Source
Minivan	Model	2008 Dongfeng EQ6362PF	Manufacturer
	Dimension [mm]	3640x1560x1925	Calculation

Table 1. Summary of the collision case [8]

Item	Category	Details	Source
Pedestrian	Mass [kg]	985	Victim
	Impact speed [km/h]	45	
	Age	40	
	Height [cm]	172	
	Weight [kg]	68	
Main injuries from primary contact	Lower limb	Right tibia shaft fracture（AIS2）	Hospital
	Thorax	Bilateral pulmonary contusion（AIS4）	
		Multiple rib fractures（AIS3）	
	Head	Concussion（AIS2）	

2.3 Computational modeling

The initial velocity of 45 km/h, which corresponds to the real world scenario, will be applied to the minivan via the research model. The right side of the pedestrian model is arranged to be oriented towards the center of the minivan. Through continuous fine - tuning of the position of the pedestrian relative to the minivan, the minivan model is deformed to a similar extent as that of the minivan in the actual accident. This deformation serves as the basis for subsequent injury analysis.

The number of nodes in the computational model is 1203337, and the number of elements is 2405592, including shell elements, solid elements, and beam elements used to connect or simulate muscles. Calculate the minimum time step and control it within

3e-4ms. The number of CPU cores used for calculation is 128. The simulation time is set to 200ms.

The simulation is set to a duration of 200 ms, during which the entire process from the moment the pedestrian is struck, to the impact of the head on the windshield, and finally to the complete detachment of the lower limbs from the minivan can be encompassed. In the course of the simulation, to cut down on computational cost, the parts of the minivan that have no contact with the pedestrian and exhibit minor deformations are removed. The parts that have direct contact with the pedestrian and undergo significant deformations are connected to the structural components. To compensate for the mass of the removed components, corresponding mass points are added to the minivan's center of mass. The mass points and the nodes of the frame with minor deformations are constrained so that the correct movement direction can be ensured.

3 Results

3.1 Kinematic Result

When compared with the actual deformation of the minivan, the deformation of the windshield in the simulated minivan is found to be lower. The deformation amplitudes of the engine hood and the front bumper are observed to be similar and are concentrated on the left side, while no substantial deformation is detected on the right side.

The injury situation of the model after the collision is approximately the same as that of the minivan in the real accident (Figure 7). It is decided that the injury prediction result of AC - HUMs can be further analyzed, and its injury - prediction ability can be evaluated.

From the kinematic results of the pedestrian collision (Figure 8, Figure 9), it can be seen that the lower limbs of the pedestrian are the first to collide with the bumper of the minivan. Subsequently, the hips, chest, and right arm of the pedestrian are made to come into contact with the engine hood. During this process, the lower limbs are gradually detached from the ground, the head is gradually made to approach the windshield and collide with it. At the same time, the lower limbs, chest, and other parts are gradually separated from the minivan. The main reasons for the deformation of the minivan model are that during the collision process, the human calf, hip, chest, shoulder, and head successively collide with the bumper, engine hood, and windshield. The main concave areas are caused by the left calf hitting the bumper, the right - side of the hip hitting the engine hood, and the right - side of the head hitting the windshield.

Fig. 7. Deformation traces in the minivan of the simulation

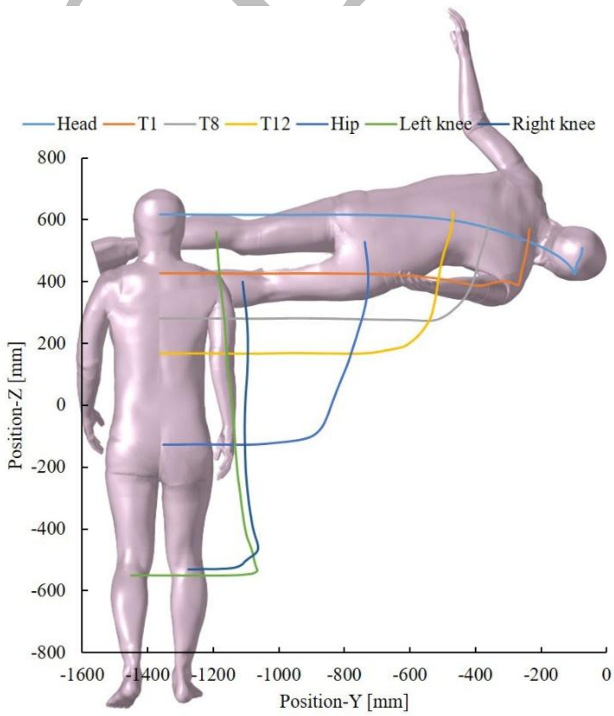

Fig. 8. Initial and final position of pedestrian model relative to minivan during collision

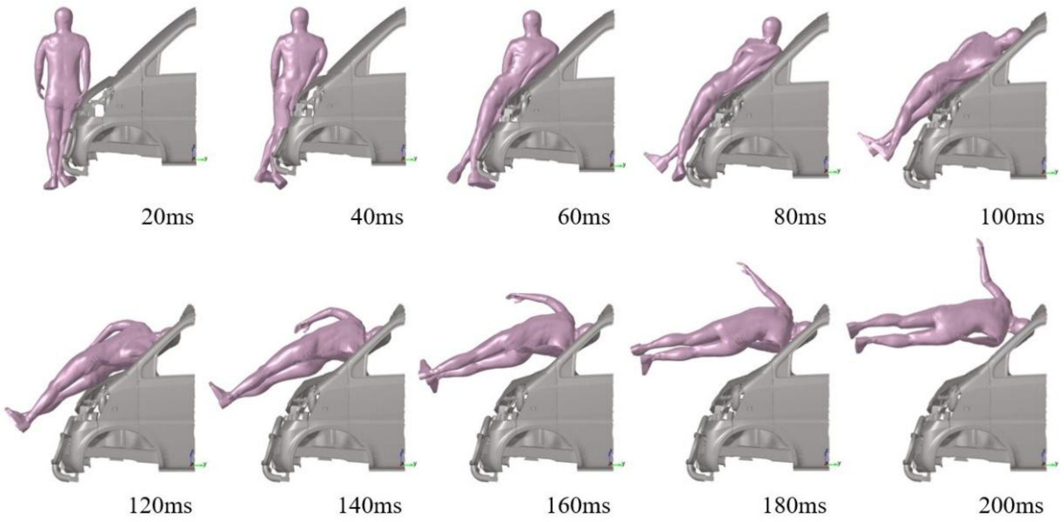

Fig. 9. Kinematic images of pedestrians and minivan during simulation

3.2 Lower Extremity Injury

For the lower limbs of AC - HUMs, a failure threshold of 129 MPa for tibia and fibula fractures and a failure threshold of 114 MPa for femur fractures are adopted, and a failure threshold of maximum principal strain of 0.24 is utilized for ligaments [17]. In the simulation, the tibia and fibula of the right lower leg are fractured (Figure 10). The predicted fracture position of the lower limb is found to be identical to that of the CT image, while the tibia and fibula of the left lower leg are not fractured. It can be inferred from the position of minivan deformation (Figure 7) that the direct cause of the fracture of the right tibia and fibula is the collision with the lower end of the bumper. The tibia is fractured at approximately 18 ms, and the fibula is fractured at around 8 ms.

During the collision event, the maximum stress borne by the tibia reached 130.2 MPa, surpassing the fracture threshold value of 129 MPa. Evidently, the prediction regarding the tibia is in accordance with the injury condition of the victim in the collision (Figure 11). Meanwhile, the peak stress of the femur did not exceed the injury threshold of 114 MPa, and thus no fracture took place.

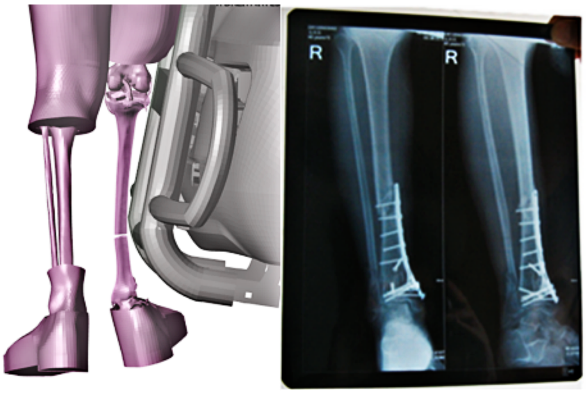

Fig. 10. Tibial fracture locations of AC-HUMs

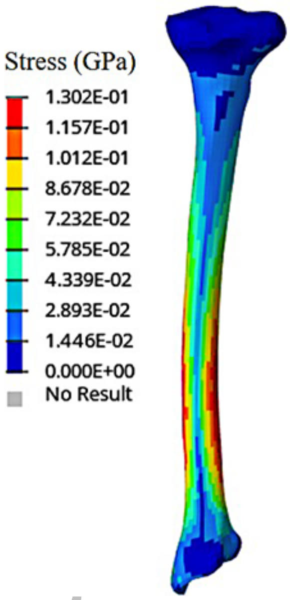

Fig. 11. Tibial fracture stress of AC-HUMs

3.3 Chest Injury

For the chest and abdomen of AC - HUMs, a maximum principal strain fracture failure threshold of 1.8% for ribs is adopted. In the simulation, the maximum principal strain values of the left sixth rib, seventh rib, eighth rib, ninth rib, tenth rib, and the right eleventh rib are all found to surpass the failure threshold [26] (1.8%) (Figure 12). It is predicted that a total of six ribs will be fractured. When compared with the CT image results, it can be observed that a total of six ribs of the pedestrian are fractured. Thus, the rib fracture result predicted by AC - HUMs is considered similar to that of the CT image.

Based on the impact position, it can be inferred that, first, the skin near the 10th - 12th ribs on the right side of the pedestrian's chest is made to strike the minivan engine hood (Figure 9), which leads to the maximum principal strain of the right eleventh rib exceeding the threshold. Subsequently, as the pedestrian's head is made to collide with the windshield and the lower limbs are detached from the ground, the ribs on the non - impact side (left side) of the chest are compressed, and the maximum principal strain of the 6th - 10th rib cortical bones is caused to exceed the threshold. The chest injury level has been determined to have reached AIS3+.

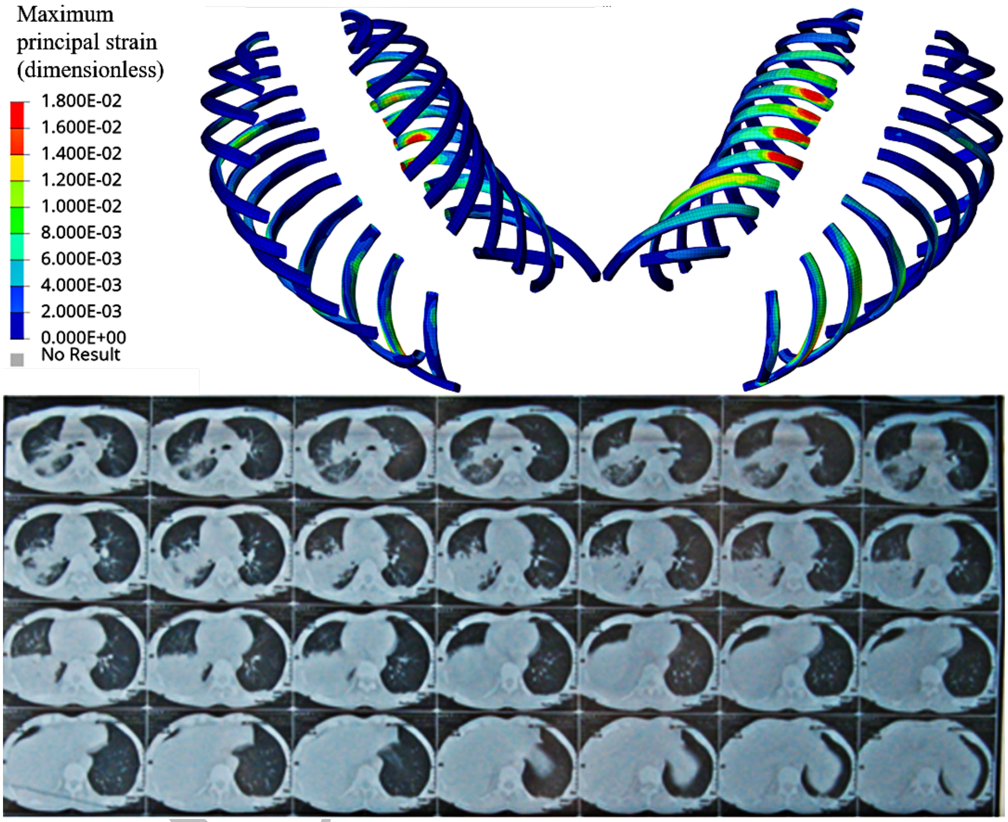

Fig. 12. Prediction of rib fracture (six rib fractures)

3.4 Head Injury

Prior to the prediction of brain tissue injuries, the biomechanical indexes of brain tissue injuries were first examined (Table 2). The intracranial pressure and maximum principal strain thresholds of brain tissue, along with the corresponding injury risks, were investigated separately.

In the context of intracranial pressure directions, positive pressure indicates compression, typically stemming from the direction where the pressure is exerted. Conversely, negative pressure denotes tension, commonly occurring on the side opposite to the area being compressed. An exceedingly high intracranial pressure can inflict damage on the brain and other associated tissues. Tension has the potential to induce deformation in the cortical layer and axons. When this tension becomes excessive, it can give rise to focal injuries and bruises [16].

The intracranial pressure and brain strain cloud maps are output by the AC - HUMs head. The results cover the pressure or strain distributions of the cerebrum, cerebellum, and brainstem. They include the peak positive pressure at the main head impact site, the peak negative pressure on the contralateral side, and the peak maximum principal strain. The strain distribution differences between the cerebrum and brainstem due to geometric disparities can be clearly observed (Figure 13). For head injuries, the intracranial pressure injury threshold and the brain strain injury threshold are adopted. The maximum positive pressure of the intracranial pressure is determined to be 238.6 kPa, which is predicted to result in a severe and fatal brain injury (AIS5 +) [21] (235 kPa). The maximum negative pressure is measured as - 170.2 kPa, which is predicted to reach an AIS3 + injury level with a 50% probability [27] (- 152 kPa) (Figure 9). The maximum strain of the brain tissue is found to be 40.046%, located in the lateral ventricle on the collision side and exceeding the concussion threshold (21%) [11] (Figure 13). In the accident report, the pedestrian injury result from the hospital indicates that the pedestrian has a slight concussion. However, all the injury predictions of AC - HUMs reach the level of concussion or moderate brain injury. When compared with the actual injury of the victim, the brain injury prediction of the Chinese human body model shows a tendency of overprediction.

Table 2. Biomechanical indexes of brain injury

Biomechanical parameter		Injury threshold	reference
Intracranial pressure (kPa)	Positive pressure	No injury:173	Ward,1980[21]
		Moderate brain injury:173~235	
		Severe and fatal brain injury:235	
		50% probability of AIS 3+ injury level:256	Yao,2008[27]
		Cerebral contusion:277	Mao,2013[11]
	Negative	50% probability of contralateral	Kleiven,2007[7]

Table 2. Biomechanical indexes of brain injury

Biomechanical parameter	Injury threshold	reference
pressure	cerebral contusion:-55.1 Severe brain injury:-186	Ward,1980[21]
	50% probability of AIS 3+ injury level:-152	Yao,2008[27]
Maximum principal strainMPS (%)	50% probability of concussion:21	Kleiven,2007[7]

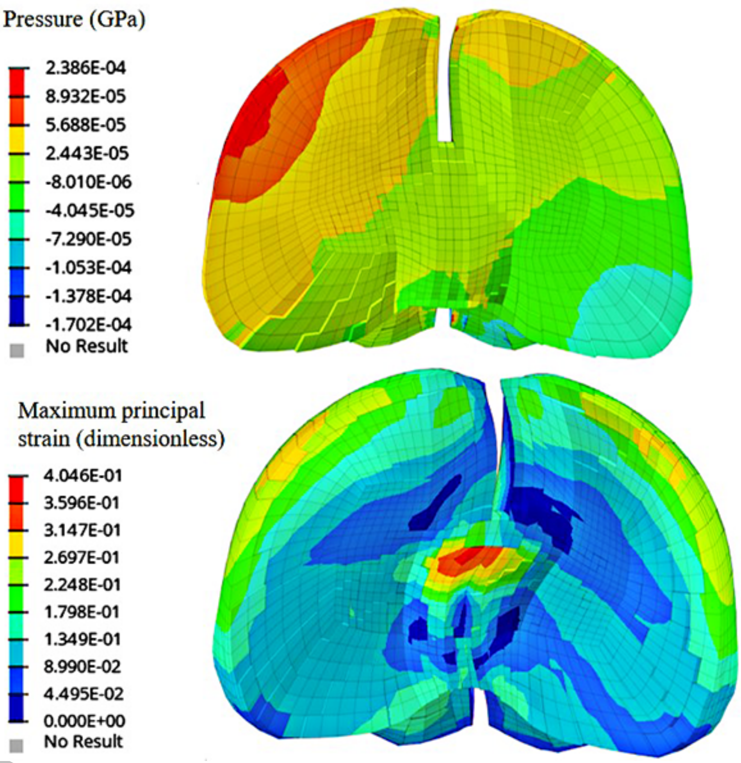

Fig. 13. Intracranial pressure stress (GPa) and brain strain results

4 Discussion

This study presents a numerical reconstruction of a pedestrian collision using the AC-HUMs 50th percentile male model, with a comparative analysis conducted on head brain injury, chest injury, and lower limb injury. The results indicate that in terms of lower limb injury prediction, discrepancies are observed between AC-HUMs and the actual injury condition of the pedestrian. While both tibia and fibula fractures are predicted in AC-HUMs, only a tibia fracture is reported in the injured individual, although the injury severity level remains unchanged. This discrepancy is hypothesized to result from differences in collision positioning, as the tibia of the pedestrian's right lower limb is positioned closer to the bumper compared to the fibula, whereas in AC-HUMs, the fibula is relatively closer to the bumper.

Regarding chest injury, this study focuses on the comparative analysis of rib cortical bone injury, which is relatively easier to evaluate. Both the model and the pedestrian are found to exhibit rib injuries at the AIS3 level. However, differences are noted in the specific locations of the injured ribs, which may be attributed to variations in collision positioning due to body shape disparities. Additionally, a partial strain concentration phenomenon is observed near the connecting hinge between the spine and the rib cage of AC-HUMs, particularly in the region of the ribs closest to the spine. This situation occurs due to the requirements of modeling the rotating joint. To model it, a layer of rigid shell elements must be added to the cortical bone at the end of the rib. Moreover, the cortical bone of the thoracic vertebra in the spine, which is in the vicinity of this area, also has a layer of rigid shell elements added. Consequently, when the end of the rib experiences a lateral impact, strain concentration is likely to happen.

In the prediction of brain injury, the injured individual is reported to have sustained a mild concussion (AIS2 level), whereas AC-HUMs predicts injuries exceeding the AIS3 level, reaching up to AIS5, indicating a significant overprediction trend. Apart from the differences in collision positioning, a key contributing factor is identified as the failure to incorporate windshield failure in the finite element model. This omission results in the head being subjected to continuous impact post-collision, potentially exacerbating the predicted injury severity.

In contrast to the research conducted by Li [9], among the components where AC - HUMs collides with the minivan, the overall deformation ranges of the windshield and the engine hood of the AC - HUMs model are determined to be smaller. Moreover, in the part where the lower limbs collide with the bumper, only one end is shown to have significant deformation. However, the bumper is caused to have significant deformations at both ends by the THUMS collision, and the deformation amplitudes at the three collision positions of the latter minivan model are all found to be considerably larger than those of the actual minivan. Evidently, when compared with THUMS, the minivan deformation obtained from the numerical reconstruction using AC - HUMs is considered more reasonable.

5 Conclusion

In this traffic collision where a minivan collided with a pedestrian, various degrees of injuries were inflicted upon the pedestrian in the lower limbs, ribs, and head. During the numerical reconstruction process that utilized the AC-HUMs model, the lower limb and chest components of AC-HUMs demonstrated good injury-prediction capabilities. When the results were compared with the actual injury conditions of the pedestrian in the real accident, the head injury prediction result derived from intracranial pressure was found to be more severe, whereas the head injury prediction result based on brain strain was found to be more consistent with the actual situation. This outcome reflects the satisfactory performance of the AC-HUMs model in reconstructing pedestrian traffic collisions.

The innovation of this study is manifested in the fact that, unlike previous injury research endeavors that relied on Western anthropometric models such as THUMS, which were designed to suit the body sizes of Western individuals, a numerical reconstruction of Chinese traffic collisions was carried out in this study. This reconstruction was based on the Chinese anthropometric model, thus distinguishing it from prior research approaches.

Conflicts of Interest

The authors declare that there is no conflict of interest regarding the publication of this paper.

References

[1] Alvarez V., Halldin P., Kleiven S., The influence of neck muscle tonus and posture on brain tissue strain in pedestrian head impacts, Stapp Car Crash Journal, 2014,

58(1):63-101, DOI: 10.4271/2014-22-0003.

[2] Chen H., Poulard D., Crandall J., Panzer M., Pedestrian response with different initial positions during impact with a mid-sized sedan, Proceedings of the 24th International Technical Conference of Enhanced Safety of Vehicles (ESV), 2015.

[3] Chen X., Huang H., Zeng D., Gao J., Ling Y., Ye B., Long Y. C., Liu Y., Research on the pedestrian head impact characteristics under low-speed conditions based on the fusion of active and passive technologies, Chinese Journal of Automotive Engineering, 2024, 1-12.

[4] Ciaran S., Pedestrian and Cyclist Impact- A Biomechanical Perspective, Springer, 2009.

[5] Euro NCAP, Euro NCAP TB024 - Pedestrian Human Model Certification v4.0. https://cdn.euroncap.com/media/66108/tb-024-pedestrian-human-model-certification-v301.pdf. Accessed 26 December 2024.

[6] Isshiki T., Konosu A., Takahashi Y., Development and evaluation of the advanced pedestrian legform impactor prototype which can be applicable to all types of vehicles regardless of bumper height-Part 1: finite element model, Proceedings of the International Research Council on Biomechanics of Injury (IRCOBI) Conference, 2016.

[7] Kleiven S., Predictors for traumatic brain injuries evaluated through accident reconstructions, Stapp Car Crash Journal, 2007, 51(81):81-114, DOI: 10.4271/2007-22-0003.

[8] Li G. B., Nie J., Yang J. K., Zhou X., Zhang C., Yu X., Li W., Wang M., A study on injuries and kinematics in pedestrian accidents involved minivan and sedan, Proceedings of the 5th International Conference on ESAR (Expert Symposium Accident Research), 2012.

[9] Li G. L., Tan Z., Lv X. J., Ren L. H., Numerical reconstruction of injuries in a real world minivan-to-pedestrian collision, Acta of bioengineering and biomechanics, 2019, 21(2):21–30, DOI: 10.5277/ABB-01342-2019-02.

[10] Li G., Yang J., Simms C., The influence of gait stance on pedestrian lower limb

injury risk, Accident Analysis & Prevention, 2015, 85(1):83-92, DOI: 10.1016/j.aap.2015.07.012.

[11] Mao H., Zhang L., Jiang B., Genthikatti V. V., Jin X., Zhu F., Makwana R., Gill A., Jandir G., Singh A., Yang K. H., Development of a finite element human head model partially validated with thirty five experimental cases, Journal of biomechanical engineering, 2013, 135(11):111002, DOI: 10.1115/1.4025101.

[12] Mizuno Y., Summary of IHRA Pedestrian Safety WG Activities, Proceedings of 19th International Technical Conference on the Enhanced Safety of Vehicles(ESV), 2005.

[13] Nie J., Li G., Yang J., A study of fatality risk and head dynamic response of cyclist and pedestrian based on passenger car accident data analysis and simulations, Traffic Injury Prevention, 2015, 16(1):76-83, DOI: 10.1080/15389588.2014.881477.

[14] Pal C., Okabe T., Vimalathithan K., Manoharan J., Shinada M., Effect of Vehicle's Front End Profile on Pedestrian's Lower Extremity Injury Pattern in Real World and Verification by Large Male FE Human Model, SAE Technical Study Series, 2015, 2015-01-1467, DOI: 10.4271/2015-01-1467.

[15] Ptak M., Pedestrian Safety: A New Method To Assess Pedestrian Kinematics, Transport, 2019, 34(1):41-51, DOI:10.3846/transport.2019.7081.

[16] Schmitt K. U., Niederer P. F., Cronin D. S., Morrison III B., Muser M. H., Walz F., Trauma Biomechanics-An Introduction to Injury Biomechanics, fifth edition, Springer, 2009.

[17] Takahashi Y., Kikuchi Y., Konosu A., Ishikawa H., Development and validation of the finite element model for the human lower limb of pedestrians, Stapp car crash journal, 2000, 44(1):335-355, DOI: 10.4271/2000-01-SC22.

[18] Toyota Motor Corporation. Total Human Model for Safety (THUMS) AM50 pedestrian/occupant model academic version 4.02_20150527 documentation.

[19] Wang B., Yang J., Otte D., Peng Y., A study of long bone fractures via reconstruction of pedestrian accident using multi-body system and lower extremity FE model, Journal of Mechanics in Medicine and Biology, 2015, 15(1):1550016.

[20] Wang G. D., Shen J. F., Zhong L. W., Reconstruction of pedestrian lower limb injury in human-vehicle collision based on THUMS model, Agricultural Equipment & Vehicle Engineering, 2022, 60(1):103-106, DOI: 10.3969/j.issn.1673-3142.2022.01.022.

[21] Ward C., Chan M., Nahum A., Intracranial Pressure-A Brain Injury Criterion, SAE Transactions, 1980, 89(1):3867-3880, DOI: 10.4271/801304.

[22] Watanabe R., Katsuhara T., Miyazaki H., Kitagawa Y., Yasuki T., Research of the Relationship of Pedestrian Injury to Collision Speed, Car-type, Impact Location and Pedestrian Sizes using Human FE model (THUMS Version 4), SAE Technical Study Series, 2012, 2012-22-0007, DOI: 10.4271/2012-22-0007.

[23] Watanabe R., Miyazaki H., Kitagawa Y., Yasuki T., Research of Collision Speed Dependency of Pedestrian Head and Chest Injuries using Human FE Model (THUMS Version 4), Proceedings of 22nd International Technical Conference on the Enhanced Safety of Vehicles (ESV), 2011.

[24] Wdowicz D., Ptak M., Numerical Approaches to Pedestrian Impact Simulation with Human Body Models: A Review, Arch Computat Methods Eng, 2023, 30:4687–4709, DOI:10.1007/s11831-023-09949-2.

[25] Wu T., Kim T., Bollapragada V., Poulard D., Chen H., Panzer M., Forman J., Crandall J., Pipkorn B., Evaluation of biofidelity of THUMS pedestrian model under a whole-body impact conditions with a generic sedan buck, Traffic Injury Prevention, 2017, 18(1):148-154, DOI: 10.1080/15389588.2017.1318435.

[26] Xiao S., Yang J. K., Xiao Z., Jeff R. C., Analysis of chest injury in frontal impact via finite element modelling based on biomechanical experiment, Chinese Journal of Theoretical and Applied Mechanics, 2017, 49(1):191-201, DOI: 10.6052/0459-1879-16-088.

[27] Yao J., Yang J., Otte D., Investigation of head injuries by reconstructions of real-world vehicle-versus-adult-pedestrian accidents, Safety Science, 2008, 46(7):1103-1114, DOI: 10.1016/j.ssci.2007.06.021.